QUALITY EVALUATION OF ADVANCED COMPOSITE STRUCTURES THROUGH LIFE CYCLE MONITORING USING EMBEDDED OPTICAL FIBER SENSORS

N. Takeda[1*], S. Minakuchi[1]

[1]*TJCC (Todai-JAXA Center for Composites), Graduate School of Frontier Sciences, The University of Tokyo, Mail Box 302, 5-1-5 Kashiwanoha, Kashiwa-shi, Chiba 277-8561, Japan*
**takeda@smart.k.u-tokyo.ac.jp*

Keywords: life cycle monitoring, optical fiber sensor, curved CFRP structures, thermal residual strains.

Abstract

This study demonstrated fiber-optic-based life cycle monitoring of an L-shaped carbon fiber reinforced plastic (CFRP) part. Fiber Bragg grating (FBG) sensors were embedded in the corner of the L-shaped specimen during the laminate lay-up process, and was then utilized to monitor the local strain change during the cure process, the demolding, the assembly, and a subsequent bending test. FBG spectral changes induced were comprehensively presented and discussed from the viewpoint of the mechanical and thermal deformation of the specimen. Internal state of the L-shaped part was successfully monitored throughout its life, confirming effectiveness of life cycle monitoring by embedded fiber-optic-based sensors for developing highly-reliable composite structures.

1 Introduction

Laminated structures made of plies of carbon fiber reinforced plastics (CFRP) have become more important over the past years for aerospace structures due to their high strength, high stiffness, low density, and corrosion resistance, among other attributes. More complicated curved shape is being fabricated. However, so-called spring-in phenomenon of curved parts is often observed which is caused by thermal residual strain mainly due to cure shrinkage and heat contraction depending on the material direction [1]. If the L-shaped part with reduced angle by the spring-in is forcibly assembled to be the right-angle, the structural strength may be significantly decreased. Furthermore, since many parameters are known or suspected to affect spring-in angle [2] in addition to the differential thermal expansion, it is difficult to prevent this phenomenon completely. Therefore, CFRP L-shaped parts can be optimized and operated safely if the internal strain changes throughout the life cycle (i.e., from the manufacturing to the operating) can be monitored in real-time. In recent years, embedded optical fiber sensing technologies have been developed. Optical fiber sensors have enough flexibility, strength, and heat resistance to be embedded relatively easily into composite laminates.

This paper demonstrates fiber-optic-based sensing for continuously monitoring the internal state of L-shaped CFRP beam. Fiber Bragg grating (FBG) sensors were embedded in the corner of the L-shaped specimen during the laminate lay-up process, and was then utilized to monitor the local strain change during the cure process, the demolding, the assembly, and a

subsequent bending test. FBG spectral changes induced were comprehensively presented and discussed from the viewpoint of the mechanical and thermal deformation of the specimen, demonstrating the life cycle monitoring technology (Fig. 1).

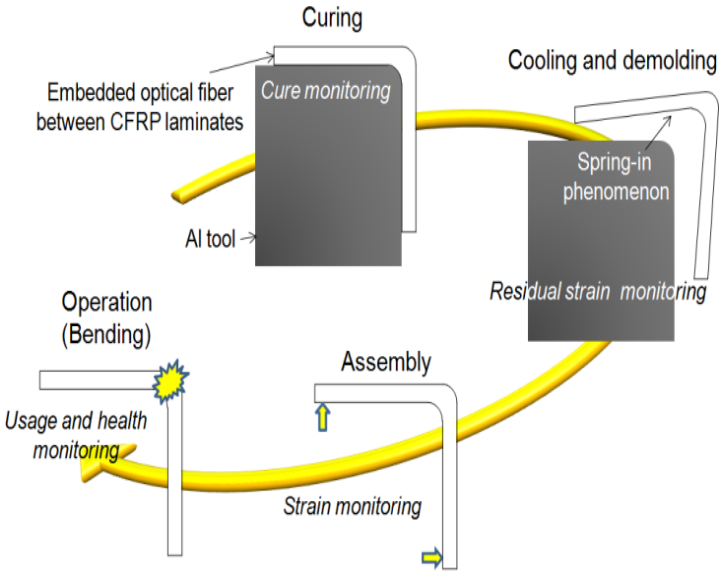

Figure 1. Schematic of life cycle monitoring of L-shaped CFRP

2 Fiber Bragg grating sensor

FBG sensors have a series of parallel gratings printed into the core of an optical fiber, and a narrow wavelength range of light is reflected from the sensors when a broadband light is illuminated. Since the wavelength at the peak of the reflected signal is proportional to the grating period, the axial strain can be measured through the peak shift (Fig. 2) [3].

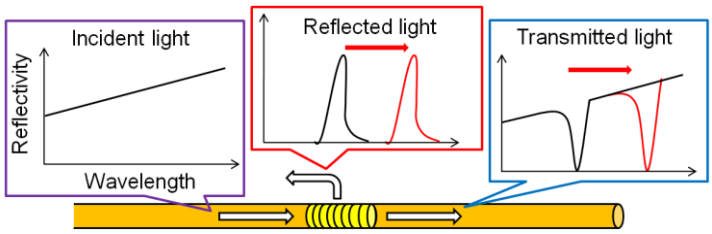

Figure 2. FBG basic sensing system

Furthermore, when a non-axisymmetric strain state arises at the core of the FBG sensor, the reflection spectrum from the sensor splits into two peaks due to a birefringence effect (Fig. 3) [4].

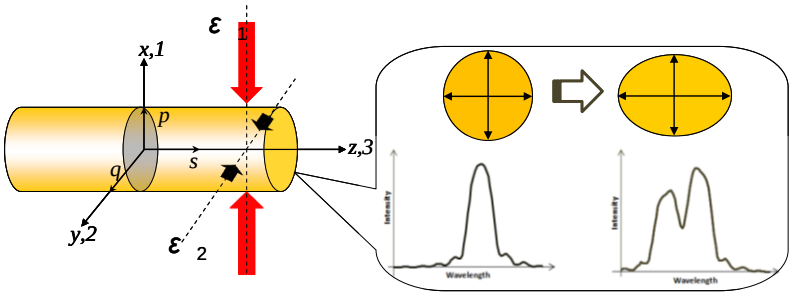

Figure 3. Sensing of non-axisymmetric strain

3 Process monitoring

3.1 Materials and methods

Figure 4 depicts a shape and size of the test specimen. It consisted of unidirectional CFRP prepreg laminates (T700S/Epoxy#2592, Toray Industries Inc., $[0_4/90_4]_{2S}$). During the lay-up process, three FBG sensors (Polyimide- coated, Fujikura Ltd., outer diameter: 150 μm, cladding diameter: 125 μm, gauge length: 10 mm) were embedded between 6-7 and 16-17 plies of the corner part, and between 16-17 plies of the flange part. The optical fiber was illuminated by an amplified spontaneous emission (ASE) light source (AQ4315A, ANDO Electric Co., Ltd.) and the reflection spectra from the FBGs were measured by an optical spectrum analyzer (AQ6331, ANDO Electric Co., Ltd.).

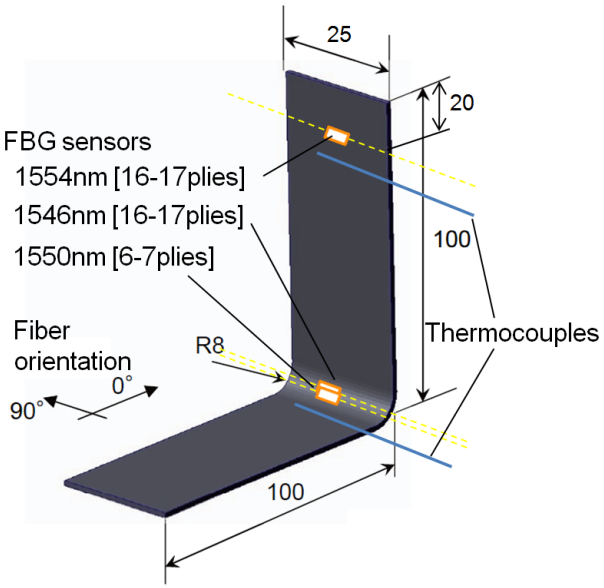

Figure 4. Design of the L-shaped specimen

In order to reduce voids in the corner part, a hot-compaction method was used during the lay-up. The specimen was cured on the Aluminum 5052 tool in an autoclave under applied pressure of 0.3 MPa. As an assistance of heating, a heat blanket was used to cover it. The schematic of the test specimen during the cure is illustrated in Fig. 5(a). Temperature cycle in the autoclave is shown in Fig. 5(b). Temperature distribution was monitored by two embedded thermocouples.

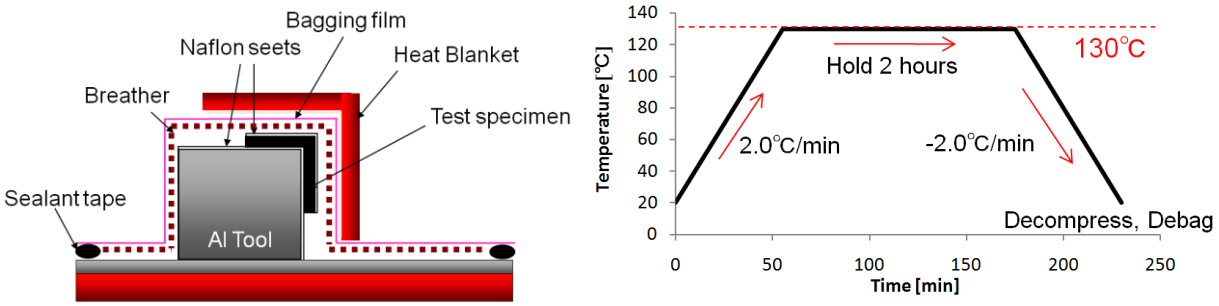

Figure 5. Schematic of test specimen during cure (a) and temperature cycle (b)

3.2 Results and discussion

Figure 6 presents the history of FBG reflection spectra during the cure cycle. During the temperature approached the maximum value (130°C), they gradually shifted to the longer

wavelength side, maintaining the initial spectral shape. In the cooling process, however, in addition to the shift back to the shorter wavelength side, the spectral shapes also changed. This phenomenon implied that non-axisymmetric strain state arose during the cooling process. In other words, the birefringence effect was introduced by thermal shrinkage. The induced strain was evaluated quantitatively. Figure 7 shows how to calculate the non-axisymmetric strain from the measured spectrum. First the difference of two peak wavelength, $\Delta\lambda$, is calculated by using the initial spectrum shape. The non- axisymmetric strain ε_d is then given by

$$\varepsilon_d = \Delta\lambda / 2k_3\lambda_0 \quad (1)$$

where λ_0 is the initial center wavelength, and k_3 (= 0.146) is the constant of optical fiber. The calculated non-axisymmetric strains were compared in Table 1. Comparing the sensors in the corner part (1546nm and 1550nm), there were no significant difference between them. However the sensor at the flange part had 40 με higher strain value than that in the corner. This is because in the flange part only thermal shrinkage occurred, while in the corner part the thermal deformation was relaxed by the mechanical strain due to the geometric restriction on the aluminum tool (Fig. 5(a)).

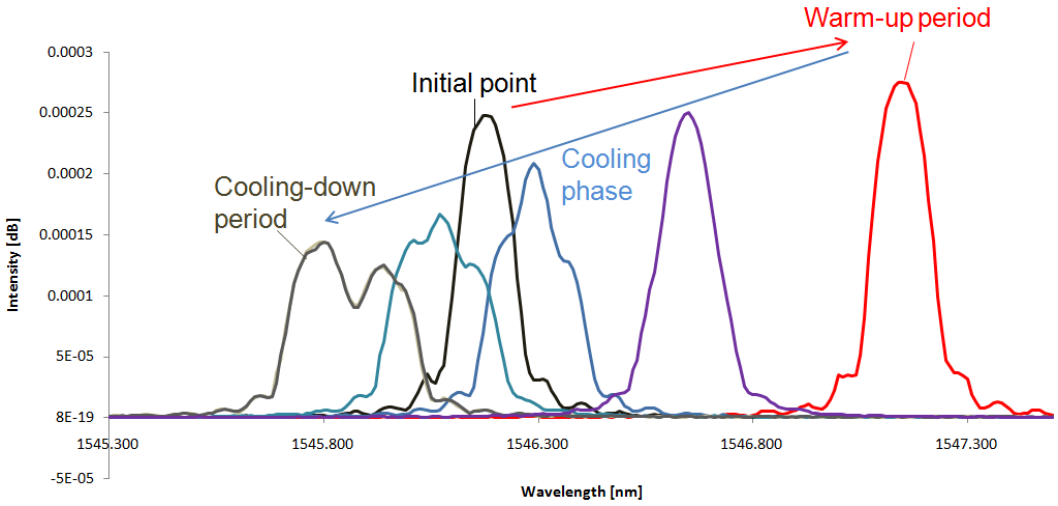

Figure 6. History of measured reflection spectra [1546nm]

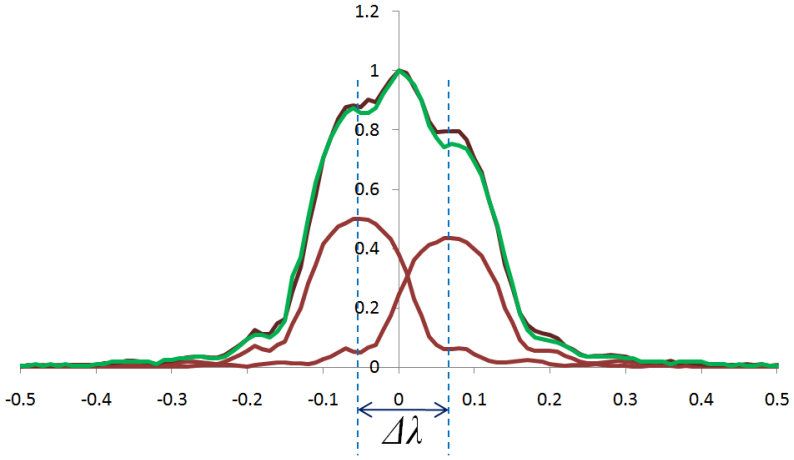

Figure 7. Calculation method of non-axisymmetryic strain

Center wavelength [nm]	Embedded place	Embedded plies	ε_d [$\mu\varepsilon$]
1546	Corner	16−17	265.821
1550	Corner	6−7	265.135
1554	Flange	16−17	308.528

Table 1. Non-axisymmetric strain ε_d

4 Four-point bending test

4.1 Methods

A four-point-bending test was conducted, and the mechanical strain was monitored by the same optical fiber used in the cure monitoring (1546nm). Figure 8 illustrates a schematic of the four-point-bending test. The specimen was loaded under the constant displacement rate of 1 mm/min. The cross-section of the corner part was inspected with a digital microscope during the test.

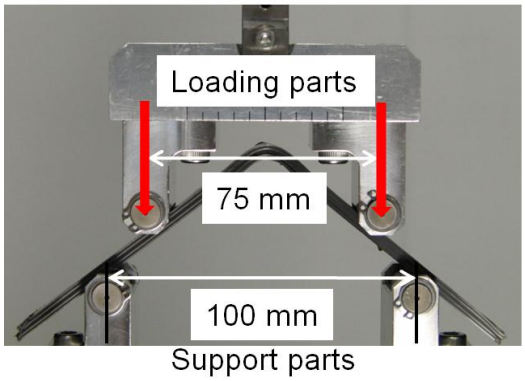

Figure 8. Four-point bending test

4.2 Results and discussion

Figures 9 (a) and (b) show the load-displacement curve and the history of normalized reflection spectra, respectively. Photographs of the corner section are presented in Fig. 10. By following the same procedure in the previous section, non-axisymmetric strains was calculated (Table 2). When the specimen moved from the state of (A) to (B), non-axisymmetric strain decreased. It indicates that through-the-thickness tensile strain occurred under the pure bending condition, counteracting the through-the-thickness compressive strain induced during the cure process. After the state of (B), the specimen failed by multiple tensile cracks along the 0^o direction at the corner part (Fig. 9 (C)). By the failure, the non-axisymmetric strain suddenly became nearly zero (Table 2). As the specimen continued to be loaded, through-the-thickness tensile strain by the bending and thus non-axisymmetric strain increased. At this time, the crack opening was significant, and it was possible to confirm the crack with the naked eye. (Fig. 9 (D)).

5 Conclusions

This study demonstrated the fiber-optic-based life cycle monitoring of L-shaped CFRP part. FBG sensors were embedded in the corner of the L-shaped specimen during the laminate lay-up process, and were then successfully utilized to monitor the cure process and the subsequent bending test. FBG spectral changes induced were comprehensively presented and discussed

from the viewpoint of the mechanical and thermal deformation of the specimen. The optical fiber could continuously monitor the internal state of the corner part, confirming that the life cycle monitoring by fiber-optic-based sensing can be used as a key technique for the development of highly-reliable composite structures.

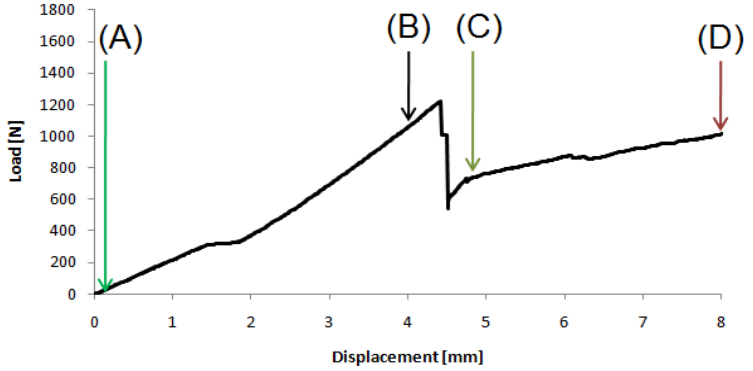

(a)

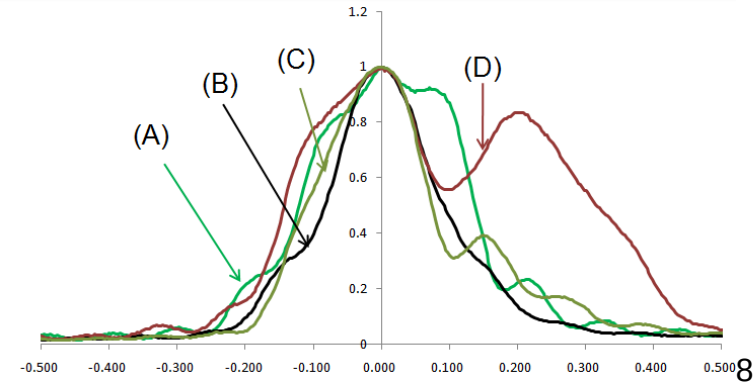

(b)

Figure 9. History normalized reflection spectra (a) and load-displacement curve (b)

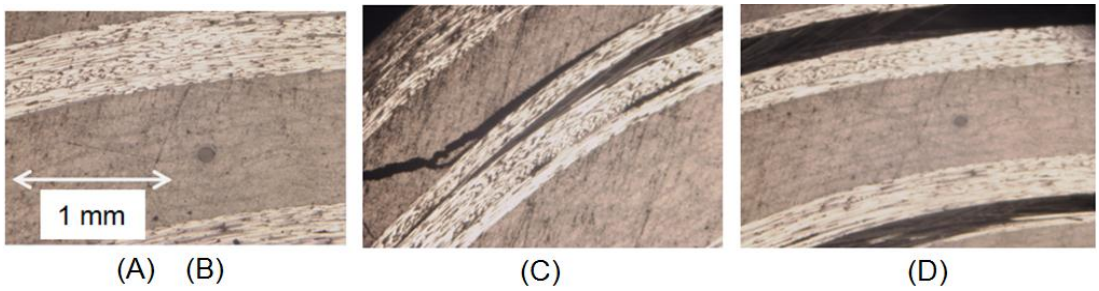

Figure 10. Photographs of corner part

State	ε_d [$\mu\varepsilon$]
A	310.124
B	177.213
C	44.346
D	487.338

Table 2. Non-axisymmetric strain ε_d

Acknowledgements
The authors acknowledge support from the Ministry of Education, Culture, Sports, Science and Technology of Japan under a Grant-in-Aid for Scientific Research (A) (No. 23246146).

References
[1] Albert, C., Fernlund, G. Spring-in and warpage of angled composite laminates. *Composites Science and Technology*, **62**, pp. 1895-1912 (2002).
[2] Wisnom, M.R., Gigliotti, M., Ersoy, N., Campbell M., Potter, K.D., Mechanisms generating residual stresses and distortion during manufacture of polymer–matrix composite structures. *Composites Part A*, **37**, pp. 522-529, (2006).
[3] Kashyap, R., *Fiber Bragg gratings*, Academic Press, San Diego, CA (1999).
[4] Minakuchi, S., Yamauchi, I., Takeda, N., Detecting an arrested crack in a foam-core sandwich structure using an optical fiber sensor embedded in a crack arrester. *Advanced Composite Materials*, **20**, pp. 419-433 (2011).